

Olfactory Ensheathing Glia Express Aquaporin 1

Shannon D. Shields,¹ Katherine D. Moore,² Patricia E. Phelps,² and Allan I. Basbaum^{1*}

¹Departments of Anatomy and Physiology and W. M. Keck Foundation Center for Integrative Neuroscience, University of California San Francisco, San Francisco, California 94158

²Department of Integrative Biology and Physiology, University of California Los Angeles, Los Angeles, California 90095

ABSTRACT

Olfactory ensheathing glia (OEG) are distinct from other glia in their developmental origin, presence in both the peripheral and central nervous systems, and highly restricted location. OEG are present only in the olfactory lamina propria, olfactory nerve, and the outer two layers of the olfactory bulb, where they envelop bundles of olfactory sensory neuron axons in a manner distinct from myelination. Because of their unique properties and their association with the continually generated olfactory sensory neurons, OEG have attracted interest for their potential capacity to support axonal regenera-

tion, for example, after spinal cord injury. However, study of the properties and function of OEG has been hampered by a paucity of neurochemical markers with which to identify and distinguish them definitively from other types of glia. Here we provide evidence through anatomical colocalization studies that OEG express the water channel aquaporin 1 (AQP1), both in vivo and in vitro. We propose that AQP1 expression represents an important distinguishing characteristic of OEG, which may impart unique function to these glia. *J. Comp. Neurol.* 518:4329–4341, 2010.

© 2010 Wiley-Liss, Inc.

INDEXING TERMS: AQP1; OEG; water channel; olfaction; lamina propria; mouse

The primary sensory neurons of the olfactory system, the olfactory receptor neurons (ORNs), are located in the olfactory epithelium that lines the nasal cavity. The superficial location of the ORNs allows for direct access to odorant molecules, but also exposes these neurons to potential damage from pollutants, microorganisms, and toxic chemicals in the environment. To maintain the integrity of the olfactory sensory apparatus, continual generation of ORNs occurs throughout the life of the animal (Graziadei and Graziadei, 1979). This feature is one of the few examples of ongoing neuronal generation in mature mammals and has been used as a model system to study renewal of neural tissue and reestablishment of functional connections after injury or disease.

From the olfactory epithelium, odorant-related information is carried in the olfactory nerve as it passes through the cribriform plate to the olfactory bulb. The olfactory nerve is composed not only of the axons of ORNs but also of the cell bodies and extensive processes of olfactory ensheathing glia (OEG). This chemically unique type of glia, with characteristics of both astrocytes and Schwann cells (Doucette, 1990), originates from the olfactory placode, not from the ventricular zone or neural crest, which is the origin of other glial cells (Valverde et al., 1992). As demonstrated in ultrastructural morphological studies,

OEG envelop or surround large groups of ORN axons along their course within the lamina propria and into the olfactory nerve and glomerular layers of the olfactory bulb (Devon and Doucette, 1992; Franklin et al., 1996; Raisman, 2001).

Because of their unique association, OEG may contribute to the ability of newly generated ORNs to project their axons past the glial limitans and form functional connections within the olfactory bulb. Recent studies have also addressed the use of OEG in studies of regeneration after complete spinal cord transection in adult rats. Indeed, some success in encouraging long-distance regrowth of transected axons and functional recovery following OEG transplantation has been reported (Ramón-Cueto et al.,

Additional supporting information may be found in the online version of this article.

Present address for S.D. Shields: Dept. of Neurology and VAMC, Yale University, West Haven, CT 06516.

The first two authors contributed equally.

Grant sponsor: National Institutes of Health (NIH); Grant numbers: NS14627, DE08377, NS54159.

*CORRESPONDENCE TO: Allan I. Basbaum, 1550 Fourth St., Box 2722, San Francisco, CA 94158. E-mail: allan.basbaum@ucsf.edu

Received January 18, 2010; Revised June 16, 2010; Accepted July 1, 2010
DOI 10.1002/cne.22459

Published online July 26, 2010 in Wiley Online Library (wileyonlinelibrary.com)

© 2010 Wiley-Liss, Inc.

1998, 2000; Lu et al., 2001, 2002; López-Vales et al., 2006; Kubasak et al., 2008).

The aquaporins (AQPs) comprise an ancient family of integral membrane proteins that function as water-selective channels in animals, plants, and microorganisms. To date, 13 mammalian AQPs have been identified (for review, see King et al., 2004). AQP1, the archetypal member of this family, is a constitutively open, bidirectional water channel expressed in red blood cells, renal proximal tubules, capillary endothelium, choroid plexus, and other tissues where water permeability is important to function (Agre et al., 2002). Recently, we also reported abundant expression of AQP1 in unmyelinated primary somatosensory neurons of the mouse (Shields et al., 2007).

In the course of our studies of the nervous system expression of AQP1, we discovered that this protein is also expressed at high levels in the olfactory bulb. Here we detail the expression of AQP1 within the olfactory system, and by comprehensive colocalization experiments demonstrate that the olfactory bulb AQP1 protein does not derive from ORNs, periglomerular cells, or astrocytes. Instead, we show that AQP1 is expressed by OEG, both in peripheral and central olfactory structures, and in olfactory bulb-derived primary cultures. We propose that AQP1 expression represents an important distinguishing characteristic of this unique glial cell.

MATERIALS AND METHODS

Animals

All animal experiments were approved by the Institutional Animal Care and Use Committees of UCSF and UCLA and were conducted in accordance with the National Institutes of Health *Guide for the Care and Use of Laboratory Animals*. AQP1^{-/-} mice (Ma et al., 1998) were originally provided by Drs. Alan Verkman and Geoffrey Manley (UCSF) and were subsequently produced by interbreeding heterozygotes. *Dlx1/Dlx2* and *Dlx5* mutant mouse embryos were a gift of Dr. John Rubenstein (UCSF). Genotyping protocols have been described elsewhere (Qiu et al., 1995, 1997; Depew et al., 1999; Shields et al., 2007).

Tissue preparation

Adult (20–30 g) male and female mice were deeply anesthetized with 100 mg/kg sodium pentobarbital and perfused transcardially with 0.1 M phosphate-buffered saline (PBS), pH 7.4, followed by 10% formalin in PBS or perfused with only phosphate-buffered (PB) 4% paraformaldehyde. Brains were collected, postfixed in the same fixative for 4 hours, cryoprotected overnight in 30% sucrose in 0.1 M PB, embedded in OCT medium (Sakura

Finetech USA, Torrance, CA), and frozen before cutting. Mice with *Dlx1/Dlx2* and *Dlx5* mutations die soon after birth, so tissue was collected from these lines at embryonic day (E)18.5 or postnatal day (P)0, and immersion-fixed in PB 4% paraformaldehyde. Olfactory bulbs, nerves, and nasal cavities were infiltrated with a series of 5–20% sucrose, incubated in 7.5% gelatin / 20% sucrose at 37°C for 1 hour, embedded in plastic molds containing the gelatin mixture, frozen in cold isopentane, and stored at –80°C. Tissue was sectioned either on a freezing microtome at 30–40 μm and processed as free-floating sections or at 20–40 μm on a cryostat and processed on slides.

Antibody characterization

Please see Table 1 for a list of all primary antisera used. The anti-aquaporin 1 (AQP1) antibody recognized expected bands in Western blot analysis from rat heart, including a 28.8-kDa band and multiple bands of higher molecular weight representing posttranslationally modified forms of the protein (manufacturer's information). Moreover, staining with this antibody was completely absent in AQP1^{-/-} mice (Shields et al., 2007; this report, Fig. 2B).

The anti-neuronal class III β-tubulin antibody recognizes a band of the expected size (50 kDa) on Western blot analysis (manufacturer's information) and stained a pattern of cellular morphology and distribution in the mouse olfactory nerve that is consistent with previous reports (Akins and Greer, 2005).

OEG were identified with three antisera: 1) The anti-p75 nerve growth factor receptor antiserum recognizes a single band at 75 kDa in Western blots of brain extracts (Huber and Chao, 1995), and stained a pattern of cellular morphology and distribution in the mouse olfactory bulb that is consistent with previous reports (Gong et al., 1994; Au et al., 2002). 2) The anti-S100 antiserum recognizes only the expected distinct double peak (S100) in a crossed immunoelectrophoresis assay of human and cow brain extracts (manufacturer's information), and revealed a pattern of cellular morphology and distribution in the mouse olfactory bulb that is consistent with previous reports (Franceschini and Barnett, 1996; Au et al., 2002). 3) Anti-rat L1 cell adhesion molecule antiserum (gift from Dr. Vance Lemmon, University of Miami) only recognizes proteins with the expected sizes of 220, 180, and 80 kDa immunoprecipitated from mouse brain extracts. This antibody does not bind to Western blots of brain membranes from L1 knockout mice (Nakamura et al., 2010).

The anti-olfactory marker protein (OMP) antibody is widely used as a reliable marker for ORNs and, in our hands, revealed a pattern of cellular morphology and distribution in the mouse olfactory bulb that is identical to

TABLE 1.
Primary Antisera Used

Antigen	Immunogen	Source & ID #	Species	Dilution
Aquaporin 1 (AQP1)	19aa synthetic peptide (aa 251-269) from the C-terminus of AQP1	Chemicon (Temecula, CA); AB3065	Rabbit polyclonal	1:8,000-10,000 or 1:60,000 (TSA)
Neuronal class III β -tubulin	Neuronal class III β -tubulin from rat brain	Covance (Berkeley, CA); PRB-435P	Rabbit polyclonal	1:10,000 (TSA)
p75-Nerve growth factor receptor (p75-NGFR)	Extracellular fragment generated from aa 43-161 of mouse p75	Chemicon (Temecula, CA); AB1554	Rabbit polyclonal	1:65,000 (TSA)
S100	S100 isolated from cow brain	Dako A/S (Glostrup, Denmark); Z0311	Rabbit polyclonal	1:2,500 (cultures) or 1:150,000 (TSA)
L1	Affinity purified L1 from rat plasma membranes	Gift from Dr. Vance Lemon (British et al., 1995)	Rabbit polyclonal	1:10,000 (cultures) or 1:500,000 (TSA)
Olfactory marker protein (OMP)	Rodent OMP	Wako (Richmond, VA); 544-10001	Goat polyclonal	1:7,500
Glial fibrillary acidic protein (GFAP)	GFAP from cow spinal cord	Dako Cytomation (Carpinteria, CA); Z0334	Rabbit polyclonal	1:2,000
Neuronal nuclei (NeuN)	Purified cell nuclei from mouse brain	Chemicon (Temecula, CA); MAB377	Mouse monoclonal	1:1,000
Tyrosine hydroxylase (TH)	Rat TH	RBI (Natick, MA); T-186	Mouse monoclonal	1:5,000

that described in a previous report (Monti-Graziadei et al., 1977).

The anti-glial fibrillary acidic protein (GFAP) antibody stains astrocytes and some ependymal cells in the central nervous system (CNS), and staining is absent from skin, connective tissue, lymphatic tissue, muscle, and gastrointestinal tract (manufacturer's information). In the mouse olfactory bulb, this antibody revealed a pattern of cellular morphology and distribution that is identical to previous reports (Bailey and Shipley, 1993).

The NeuN antibody is widely used as a marker of neuronal nuclei and, in our hands, revealed a pattern of cellular morphology and distribution in the mouse olfactory bulb that is identical to previous reports (Mizrahi et al., 2006).

The anti-tyrosine hydroxylase (TH) antibody recognizes a single band of 60 kDa in Western blot analysis of PC12 rat pheochromocytoma cells (manufacturer's information) and revealed a pattern of cellular morphology and distribution in the mouse olfactory bulb that is identical to previous reports (Halasz et al., 1977; Mizrahi et al., 2006).

Immunohistochemistry

Immunohistochemical experiments were performed as previously described (Runyan et al., 2005; Shields et al., 2007; Runyan and Phelps, 2009). Species-appropriate biotinylated (1:200; Vector, Burlingame, CA) or fluorescent (1:700; Molecular Probes, Eugene, OR) secondary antibodies were used.

To further amplify AQP1 immunoreactivity we used a Tyramide Signal Amplification kit (NEL704A, Perkin-

Elmer, Boston, MA) following the manufacturer's protocol, but altered reagent concentrations and incubation times. After quenching endogenous peroxidase with 0.3% hydrogen peroxide and 0.1% sodium azide for 30 minutes, sections were incubated overnight with rabbit anti-AQP1 (1:60,000), washed with TNT buffer (0.1 M Tris-HCl, 0.15 M NaCl, 0.3% Triton X-100, pH 7.5) between steps, incubated in biotinylated goat anti-rabbit IgG (1:1,000; Vector) for 1 hour, and streptavidin-conjugated horseradish peroxidase (1:150; Perkin-Elmer) for 30 minutes. Sections were incubated in fluorophore-labeled tyramide (1:150; Perkin-Elmer) for 5 minutes and rinsed thoroughly. Before application of a second rabbit primary antiserum, sections were fixed for 15 minutes in 4% paraformaldehyde, rinsed and boiled in 10 mM citric acid buffer (pH 6.0) using a 1250W microwave for 3 minutes on 100% power followed by 2.5 minutes on 50% power (adapted from Tóth and Mezey, 2007). This step prevents unwanted specific binding of the biotinylated anti-rabbit IgG used to localize the second marker to the rabbit anti-AQP1 primary antibody (Tóth and Mezey, 2007). After the slides cooled for 30 minutes in citric acid buffer, they were rinsed in TNT buffer before initiating the second immunohistochemical reaction.

To confirm colocalization and exclude the possibility of antiserum crossreactivity, we conducted control experiments on sections from wildtype and *AQP1* null mice. Nearby sections were processed for single-labeling to compare the localization pattern and then the double-labeling procedure was conducted, except that the second primary antiserum was eliminated (see Supporting Information material).

Primary culture of OEG

Primary cultures derived from the outer two layers of mouse olfactory bulbs were prepared using methods adapted from Ramón-Cueto, et al. (2000) and identical to those reported in Runyan and Phelps (2009). Cells were fixed with 4% paraformaldehyde for 15 minutes and stored at 4°C in PB with 0.06% sodium azide until processing.

Image acquisition and processing

Digital images were captured using a CCD camera attached to either a Nikon Eclipse or a Zeiss AxioScope 2 microscope. A Zeiss LSM510 confocal microscope was used for colocalization studies. Images were assembled using Adobe Photoshop (San Jose, CA), adjusting brightness and contrast as appropriate.

RESULTS

AQP1 is expressed in the mouse olfactory bulb

We observed AQP1-like immunoreactivity (IR) in sagittal sections through the whole mouse brain. In this view (Fig. 1A), positive immunoreactivity for AQP1 is apparent in the trigeminal nucleus caudalis (the medullary homolog of the spinal cord dorsal horn; see Shields et al., 2007), the choroid plexus (where it has previously been described by Nielsen et al., 1993), the outer surface of the main olfactory bulb (Fig. 1A–E), and within the accessory olfactory bulb (Fig. 1D, inset). We did not detect IR in the brains of mice with a deletion of the AQP1 gene (Fig. 2B and data not shown). Examination of coronal sections at higher magnification shows AQP1 expression in the olfactory nerve layer (ONL) and in the glomerular layer (GL), which comprise the outer two layers of the olfactory bulb (Fig. 1B,C). Often we observed a dense meshwork of tubular-shaped AQP1 immunoreactive profiles within the inner and outer ONL (Fig. 1D,E). AQP1-positive processes in the inner ONL extend into the GL, but never enter individual glomeruli.

AQP1 is expressed in the lamina propria of the nasal cavity

We next asked if AQP1 is expressed in the two layers of the olfactory mucosa that line the nasal turbinates, the olfactory epithelium and the lamina propria. The ORN cell bodies and odorant detecting processes are found within the olfactory epithelium, while the ORN axons travel in the lamina propria where they are surrounded by OEG. We examined E18.5 wildtype and AQP1^{−/−} nasal cavities and found that AQP1 is, in fact, robustly expressed throughout the wildtype lamina propria (Fig. 2A); the lamina propria of AQP1 null mutants is blank (Fig. 2B). Wild-

type AQP1-positive cells surround unlabeled circular spaces (Fig. 2C, arrows) within the lamina propria. To determine if these spaces contain ORN axons, we double-labeled nasal cavity sections with AQP1 and the neurofilament marker β -tubulin and found axon bundles closely associated with AQP1-positive structures (Fig. 2D, arrowheads). The AQP1-positive structures that are directly apposed to β -tubulin-positive axons have a morphology consistent with peripheral OEG. Most likely other structures contribute to the heavy AQP1 expression in the lamina propria, including the perineurium, a connective tissue layer made up of epithelial cells joined by tight junctions that forms the blood–nerve barrier (Shantheraveerappa and Bourne, 1962; Thomas, 1963; Matsuzaki et al., 2005; Ablimit et al., 2006). In addition, the isolated AQP1-positive tubular structures in the olfactory epithelium (Fig. 2C, arrowheads) may be the ducts of Bowman's glands. Together, these results suggest that several populations of peripheral cells express AQP1, but only OEG are also found within the AQP1-positive layers of the olfactory bulb (Fig. 1).

AQP1 is expressed by chemically identified OEG in the main olfactory bulb

OEG surround axons of ORNs as they course from the lamina propria into the olfactory bulb and are located throughout the ONL and within the GL (Doucette, 1984, 1993; Pixley, 1992; Ramón-Cueto and Avila, 1997). To determine if the AQP1-expressing processes in the olfactory bulb belong to OEG, we performed colocalization experiments with AQP1 and three OEG markers: the low-affinity nerve growth factor receptor p75, the glial calcium-binding protein S100, and the L1 cell adhesion molecule.

The low-affinity nerve growth factor receptor p75 (p75-NGFR) is an established marker of cultured OEG (reviewed in Ramón-Cueto and Avila, 1998) and is detected early in development (Gong et al., 1994). However, soon after birth p75-NGFR expression is downregulated; only limited levels persist in the outermost ONL and GL of the adult (Gong et al., 1994; Au et al., 2002). We found p75-NGFR immunoreactivity in the outer ONL, where it colocalized with AQP1 immunoreactivity (Fig. 3A1–3, arrows), and also within the glomeruli, a region that never contained AQP1 IR (arrowheads). The limited colocalization of AQP1 and p75-NGFR is consistent with the small number of adult OEG that express p75-NGFR in vivo.

Previous studies demonstrated that OEG within the ONL, GL, and olfactory nerve express S100 (Franceschini and Barnett, 1996; Au et al., 2002), as do astrocytes (Matus and Mugal, 1975; Haan et al., 1982). As shown in Figure 3B1–3, AQP1 colocalizes extensively with S100-

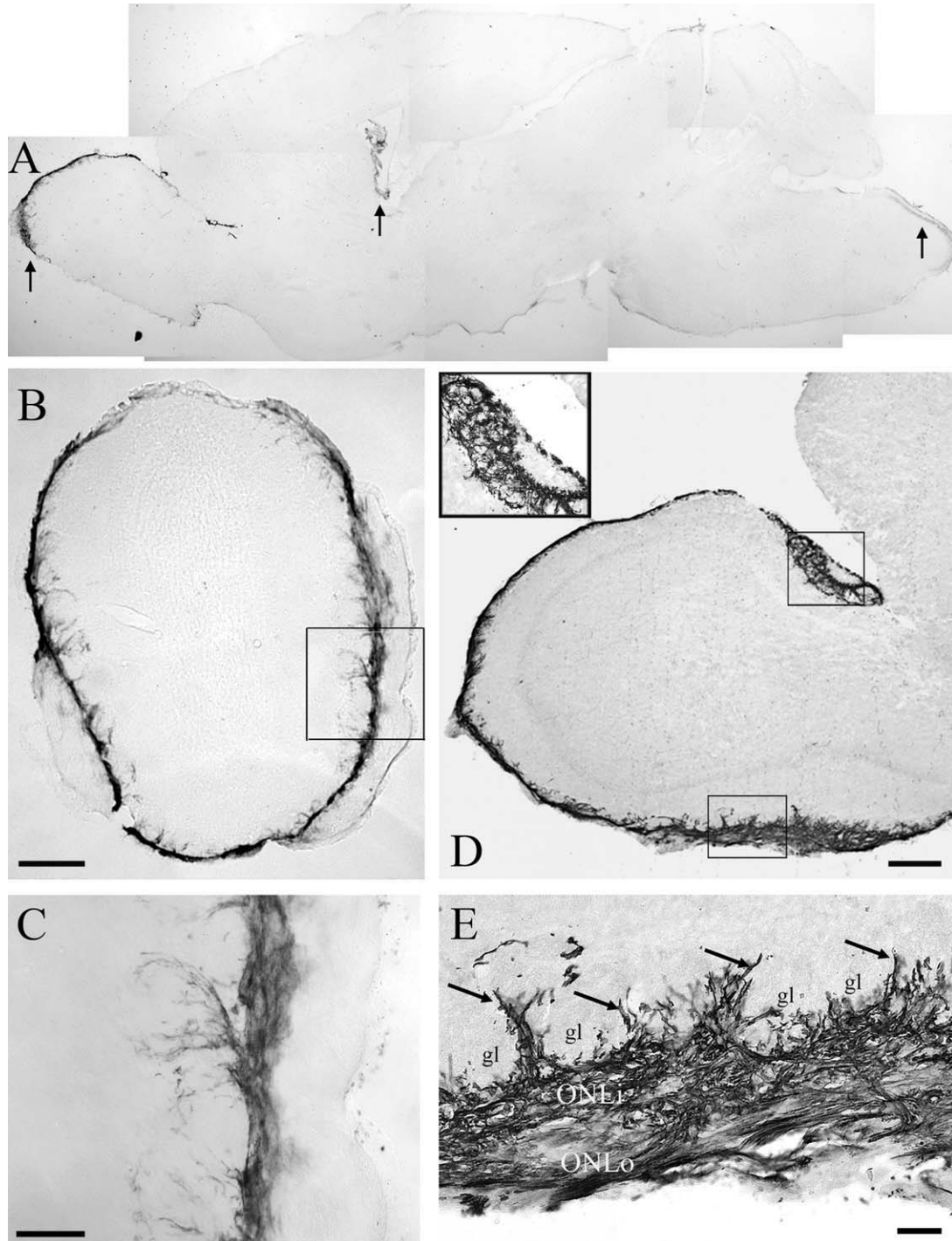


Figure 1. AQP1 IR in mouse olfactory bulb. **A:** Sagittal section through the brain shows that AQP1 IR is restricted to the trigeminal nucleus caudalis, choroid plexus, and olfactory bulb (arrows). **B:** Coronal section through the olfactory bulb shows that AQP1 IR forms a dense meshwork that surrounds the entire bulb at its external surface. **C:** Higher magnification of the boxed region in B highlights the glomerular layer AQP1 IR. **D:** AQP1 IR in a sagittal olfactory bulb section. Inset: higher magnification of the upper boxed region in D shows detail of AQP1 expression in the accessory olfactory bulb. **E:** Higher magnification of the lower boxed region in D. AQP1-positive tubular-shaped structures fill the inner (ONLi) and outer ONL (ONLo) and project (arrows) between the glomeruli (gl). Scale bars = 400 μm in B,D; 50 μm in C,E.

labeled processes in the ONL and GL, except for the nuclei (arrowheads), which immunolabel only for S100. To control for antiserum crossreactivity we first labeled

nearby sections with AQP1 and S100 individually to confirm similar expression patterns (Supporting Information Fig. 1A,B). We also performed double-labeling in the

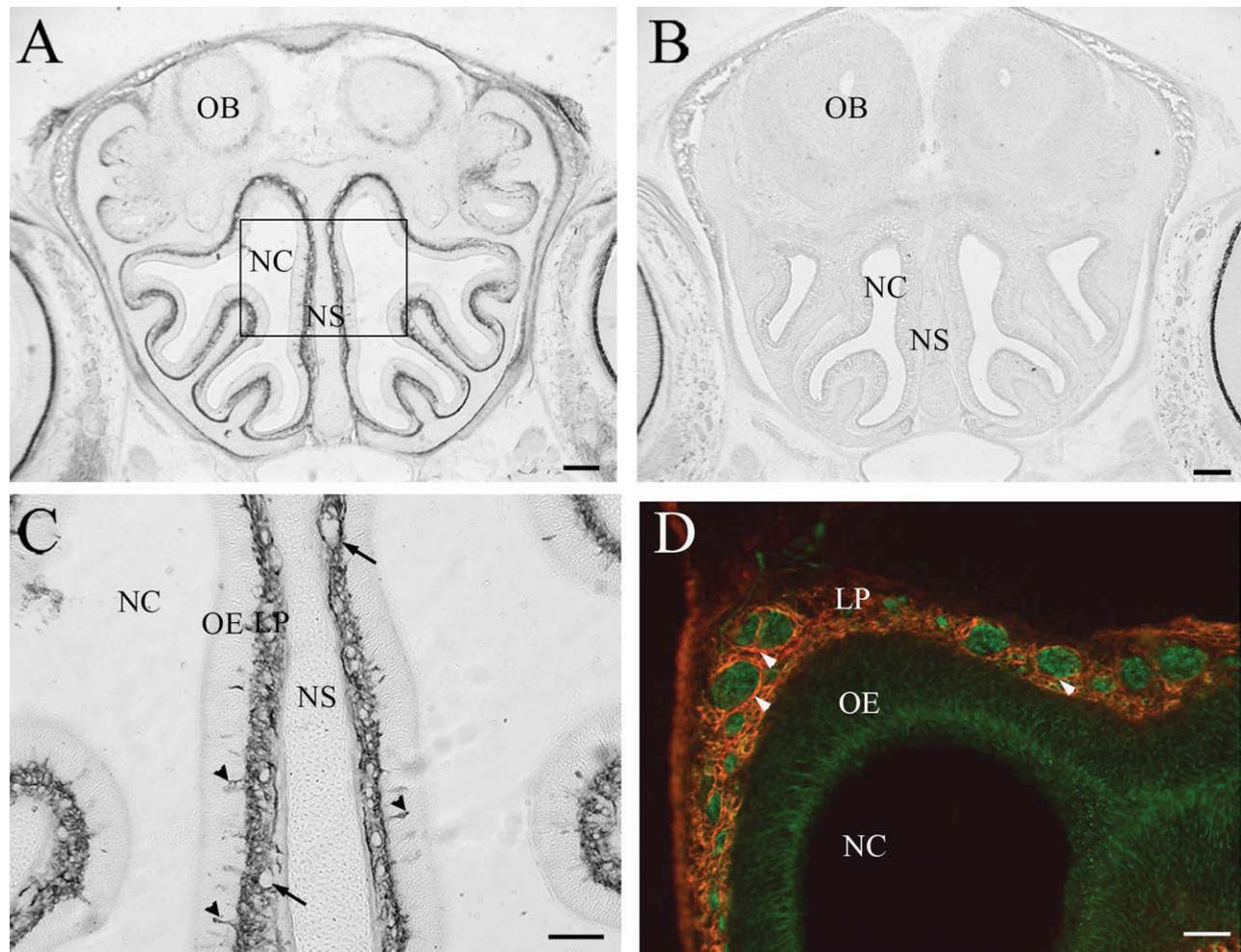


Figure 2. AQP1 in embryonic nasal cavity. **A,B:** AQP1 IR is present in the lamina propria of E18.5 wildtype mice (**A**) but is absent in AQP1^{-/-} mice (**B**). **C:** The lamina propria contains AQP1-negative circular structures (arrows) that are presumed to be bundles of ORN axons. Tubular structures likely to be the ducts of Bowman's glands are also positive for AQP1 IR (arrowheads). **D:** AQP1 IR structures (red, arrowheads) encircle axon bundles labeled for β -tubulin (green). This is consistent with OEG expression of AQP1. LP, lamina propria; NC, nasal cavity; NS, nasal septum; OB, olfactory bulb; OE, olfactory epithelium. Scale bars = 200 μ m in **A,B**; 100 μ m in **C**; 50 μ m in **D**. A magenta-green version of this figure is available as Supporting Information. [Color figure can be viewed in the online issue, which is available at wileyonlinelibrary.com.]

absence of the second primary antiserum (Supporting Information Fig. 1C,D). Results from these experiments confirm that the AQP1 and S100 antisera do not crossreact. AQP1 and S100 also colocalize in cross-sections of the olfactory nerve near its entry into the bulb (Fig. 3C1–3). AQP1- and S100-positive processes ensheath the fine olfactory nerve fascicles (between arrows), in the characteristic pattern reported by Field et al. (2003). These findings suggest that OEG express AQP1, but do not differentiate OEG from S100-expressing astrocytes.

L1 CAM is a molecule expressed by both ORN axons (Gong and Shipley, 1996) and OEG (Miragall et al., 1989; Runyan and Phelps, 2009), but not by other CNS glia. Therefore, to confirm that the S100-labeled cells in the ONL are OEG and not astrocytes, we examined the extent of overlap of AQP1 and L1 distribution. AQP1 colocalized

with some L1-positive structures in the ONL as well as with processes that surround individual glomeruli (Fig. 3D1–3, arrows). Structures labeled with L1 only are found within the glomeruli, where OEG are excluded, and adjacent to double-labeled structures in the ONL (Fig. 3D2–3, arrowheads). As OEG are the only cell type in the ONL that expresses both L1 and S100, our finding that AQP1 colabels with both of these markers strongly suggests that central OEG are the major source of AQP1 in the olfactory bulb.

Presence of AQP1-positive cells in primary olfactory bulb cultures

OEG can be cultured from the outer two layers of the adult olfactory bulb. Indeed, after culturing these OEG have been immunopurified and transplanted into the

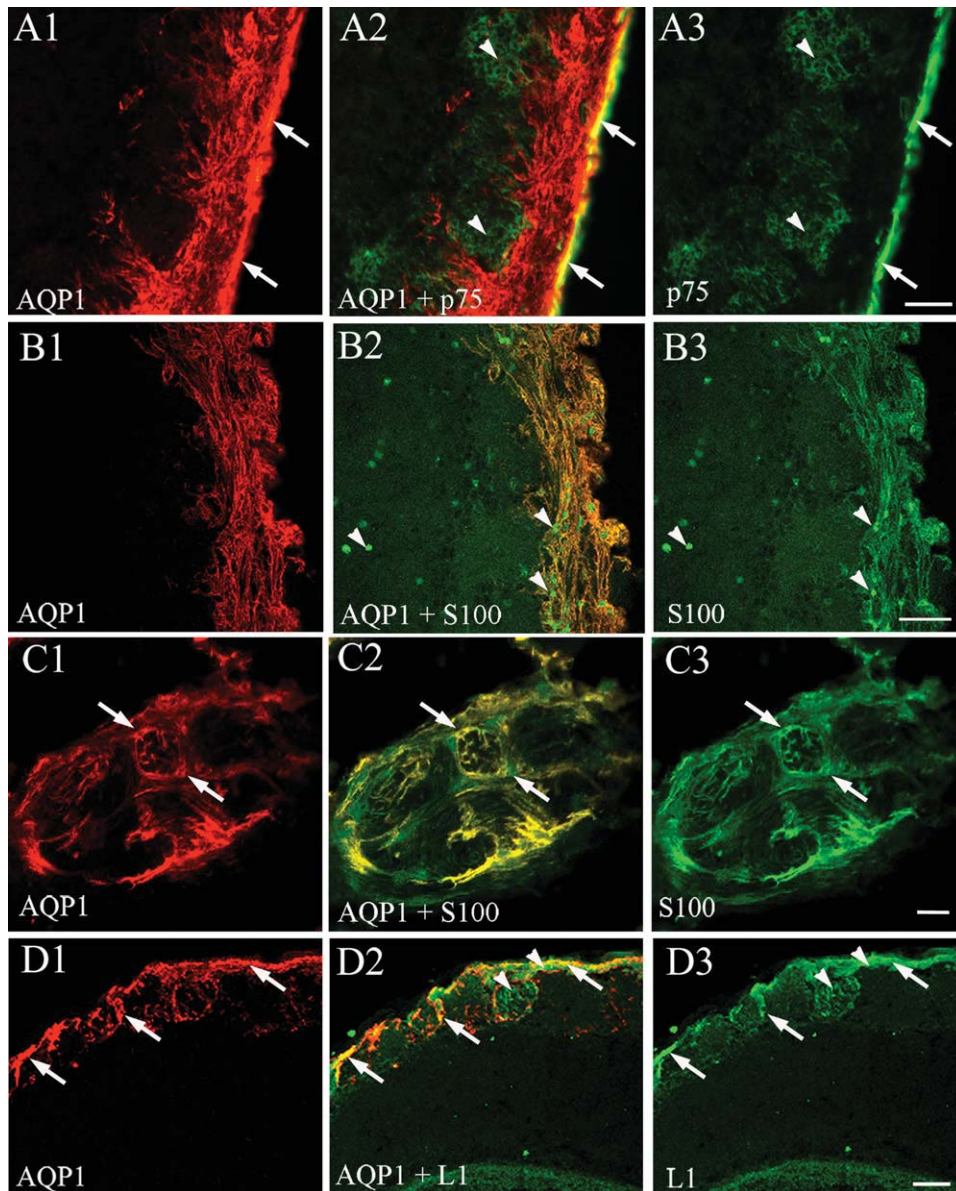


Figure 3. AQP1 IR colocalizes with OEG markers in the olfactory bulb (A,B,D) and nerve (C). **A:** p75-NGFR only colabels with AQP1 along the edge of the ONL (arrows). Individual glomeruli contain p75-NGFR (arrowheads) but no AQP1 IR. **B:** The olfactory nerve layer contains both AQP1 and S100 IR. S100-labeled nuclei (arrowheads) are negative for AQP1. **C:** AQP1 and S100 colocalize in processes that surround a fascicle of the olfactory nerve (between arrows). **D:** L1 identifies ORN axons, OEG, and unmyelinated axons deep in the olfactory bulb. Arrowheads indicate L1 single-labeled ORN axons in glomeruli and ONL; arrows identify L1 and AQP1 double-labeled structures around the glomeruli and in the ONL. OEG are the only cell type in the ONL and GL that express both L1 and S100. Scale bars = 50 μ m in A,B,D; 20 μ m in C. A magenta-green version of this figure is available as Supporting Information. [Color figure can be viewed in the online issue, which is available at wileyonlinelibrary.com.]

injured spinal cord so as to facilitate functional recovery (Ramón-Cueto et al., 1998, 2000; Lu et al., 2001, 2002; López-Vales et al., 2006; Kubasak et al., 2008). To determine if AQP1 is expressed by OEG in vitro, we prepared primary cultures from adult mouse olfactory bulbs. Figure 4A,B illustrates that a subset of spindle-shaped cells in primary cultures express AQP1. However, many of the cultured cells are marked only by nuclear DAPI labeling. Although cells were immunopositive using both the stand-

ard ABC (Fig. 4A) and TSA (Fig. 4B) kits, the TSA protocol increased the intensity of AQP1, even at a 7-fold lower primary dilution. Importantly, spindle-like cells similar to those labeled with AQP1 expressed other OEG markers, including L1 (Fig. 4C) and S100 (Fig. 4D). Based on the morphological similarities in size, shape, and number of labeled cells in wells derived from the same olfactory bulb cultures, we suggest that the AQP1-, S100-, and L1-labeled cells are OEG.

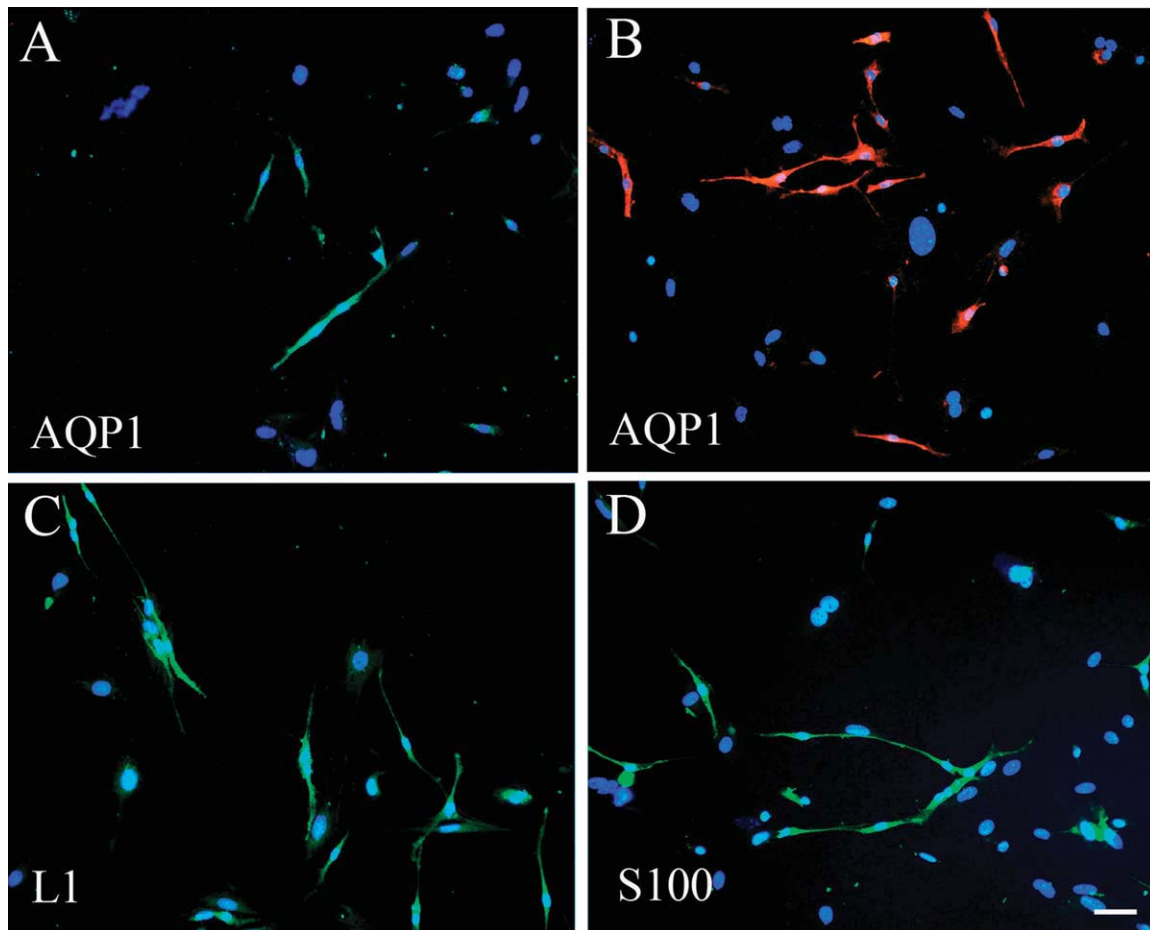


Figure 4. Primary cultures of mouse olfactory bulb contain AQP1-positive cells that we detect using standard immunofluorescent techniques (A) or after TSA amplification (B). The morphology of AQP1-labeled cells is similar to that of L1-positive (C) and S100-positive (D) cells from the same primary cultures. Nuclear DAPI staining (blue) reveals the presence of many AQP1-negative cells. Scale bar = 50 μ m. [Color figure can be viewed in the online issue, which is available at wileyonlinelibrary.com.]

AQP1 is not expressed by olfactory receptor neurons, astrocytes, or periglomerular cells

To determine if AQP1 IR in the olfactory bulb derives exclusively from the OEG, we used immunohistochemistry to localize markers of the various neuronal and glial elements that comprise the bulb. We first investigated ORNs, the sensory afferents that transmit olfactory stimuli to the brain. As for AQP1, IR for the ORN marker olfactory marker protein (OMP) is present in a dense band of fibers at the external surface of the bulb (Margolis and Tarnoff, 1973; Monti-Graziadei et al., 1977). However, in contrast to the OMP-positive fibers, which terminate exclusively within the sharply defined borders of glomeruli, AQP1-positive processes course between glomeruli, in a pattern clearly distinct from that of OMP (Fig. 5A–C).

Next, we wanted to exclude definitively olfactory bulb astrocytes as a source of AQP1 IR. As described previously (Bailey and Shipley, 1993), GFAP-positive astrocytes are located in all layers of the olfactory bulb, and are most densely concentrated in the GL. Our immunohis-

tochemical experiments show that AQP1 and GFAP IR co-occur in the GL and ONL, but in patterns that are clearly distinct (Fig. 5D,E). Specifically, AQP1 is located in long, thin processes at the superficial edge of the GL and in the ONL, while intense GFAP immunoreactivity is concentrated in the relatively short processes of stellate-shaped cells located deeper in the bulb. Based on these distinct staining patterns we conclude that AQP1 IR does not derive from olfactory bulb astrocytes.

Periglomerular (PG) cells are a type of local circuit interneuron with small cell bodies that surround the glomeruli. They interact with axons of ORNs as well as with dendrites of mitral/tufted cells (Kosaka et al., 1998). To determine whether PG cells could be a source of the AQP1 IR in the olfactory bulb, we performed immunohistochemical colocalization studies using NeuN (a pan-neuronal marker) and TH, both of which label PG cells (Halasz et al., 1977; Mullen et al., 1992). Figure 6A–F illustrates that neither marker colocalizes with AQP1 IR. We next analyzed tissue from *Dlx1/Dlx2* double mutant mice, which

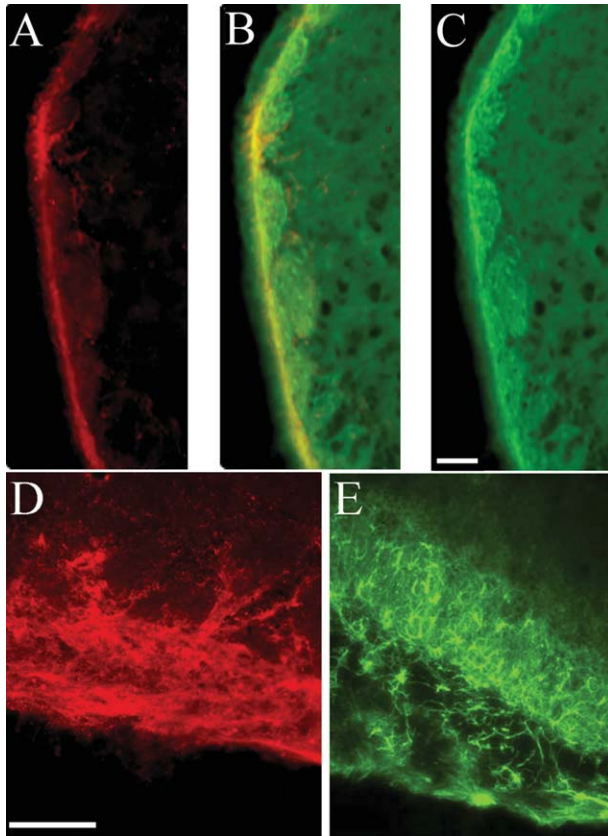


Figure 5. AQP1 IR in the olfactory bulb does not derive from ORNs or astrocytes. A–C: AQP1 and OMP are both expressed in a dense band of fibers in the olfactory nerve layer. OMP fibers (C) clearly innervate glomeruli, but the AQP1-positive fibers (A) course between glomeruli, in a pattern distinct from OMP. B: Merged image of A,C. D,E: Sections of the olfactory bulb stained for AQP1 (D) and the astrocyte marker GFAP (E) reveal distinct patterns of labeling. Scale bars = 100 μ m. A magenta-green version of this figure is available as Supporting Information. [Color figure can be viewed in the online issue, which is available at wileyonlinelibrary.com.]

have a very specific developmental defect of the olfactory bulb: despite having a normal laminar organization of the bulb, normal axonal projections from the bulb to other regions, and an intact olfactory topographic map, the periglomerular and granule cells of these mice never develop (Anderson et al., 1997; Bulfone et al., 1998). As illustrated in Figure 6G–J, we found AQP1 IR to be intact in *Dlx1/Dlx2* mutant mice compared to their wildtype littermates. We conclude that AQP1 is not expressed in PG cells.

***Dlx5* mutant olfactory bulbs have minimal AQP1 expression**

In the absence of the *Dlx5* homeobox gene, the olfactory bulbs are significantly reduced in size, the nasal cavities are malformed, and ORN axons and OEG cannot cross the cribriform plate to enter the CNS (Long et al.,

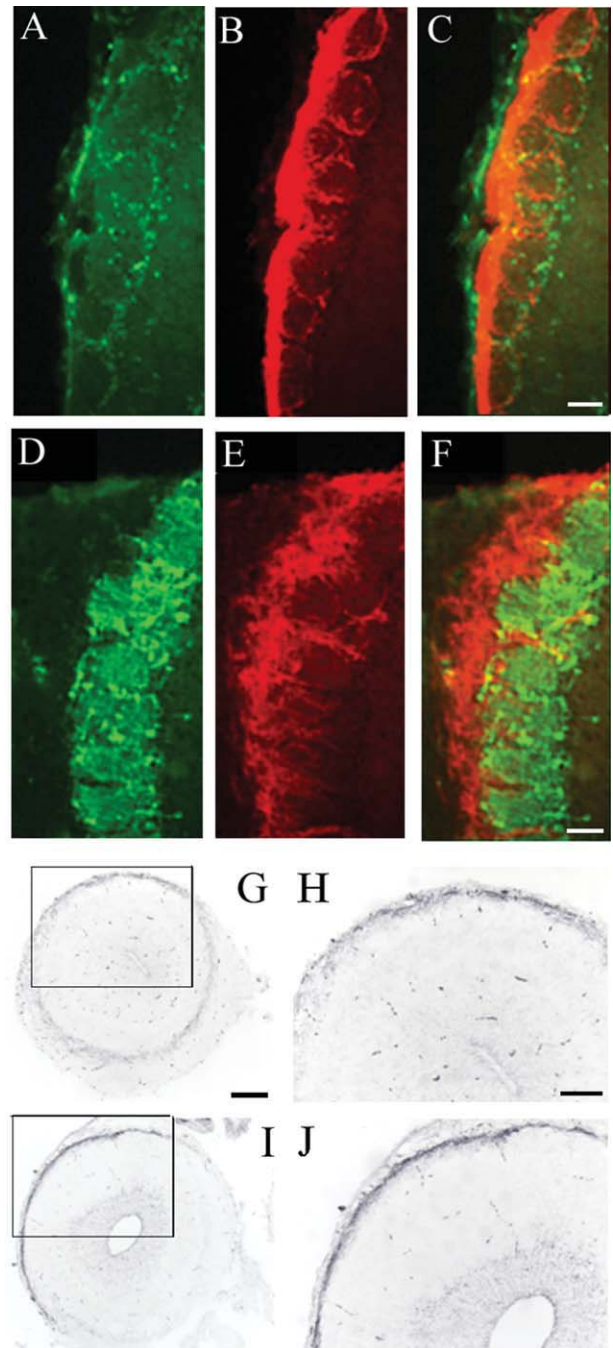


Figure 6. AQP1 IR in the olfactory bulb does not derive from periglomerular (PG) cells. A–C: AQP1 (B) does not colabel with NeuN (A), a marker of neuronal cell bodies. C: Merged image of A,B. D–F: AQP1 (E) does not colabel with tyrosine hydroxylase (TH; panel D), a marker of PG cells. F: Merged image of D,E. G–J: AQP1 staining in the olfactory bulbs of *Dlx1/Dlx2* mutant mice at E18.5 that lack PG cells (I,J) does not differ from that seen in littermate controls (G,H). Scale bars = 50 μ m in C (applies to A–C) and F (applies to D–F); 500 μ m in G (applies to G,I); 200 μ m in H (applies to H,J). A magenta-green version of this figure is available as Supporting Information. [Color figure can be viewed in the online issue, which is available at wileyonlinelibrary.com.]

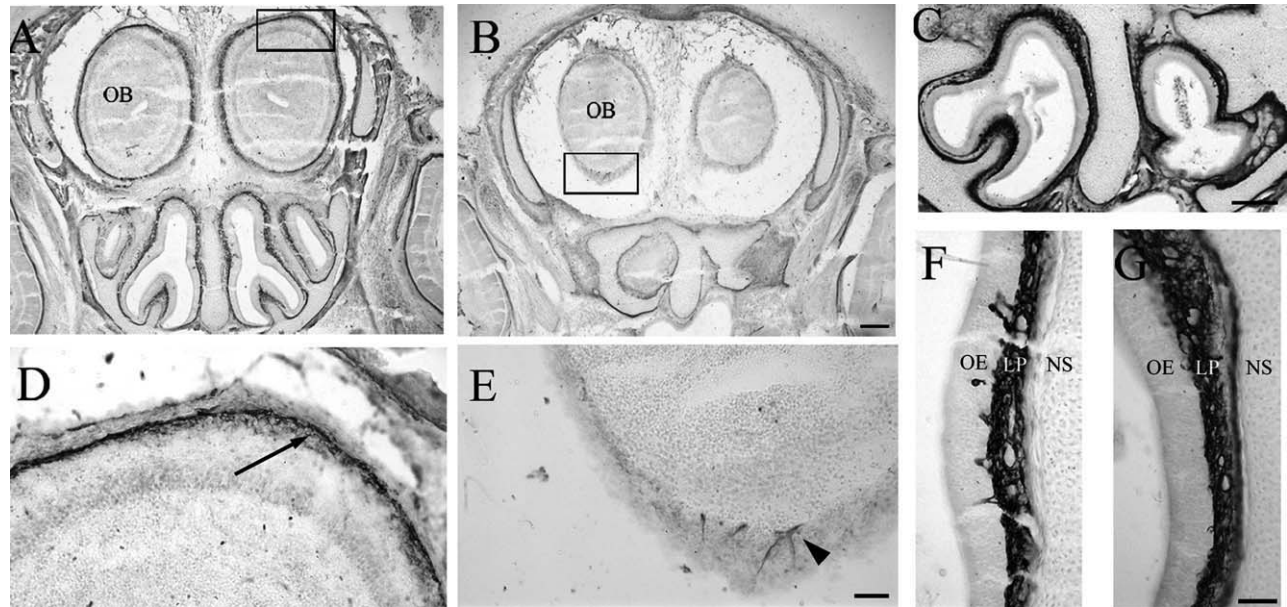


Figure 7. E18.5 olfactory bulbs of *Dlx5* mutants lack AQP1 expression. **A:** AQP1 IR is located in the olfactory bulbs (OB) and lamina propria (LP) in wildtype mice. **B:** *Dlx5* mutant OBs, which lack innervation by ORNs and OEGs, are almost completely devoid of AQP1 labeling. **C:** AQP1 IR is still present in *Dlx5*^{-/-} lamina propria, despite significant malformation of the nasal turbinates. **D,E:** Higher magnification of the boxed regions in **A** and **B** show that AQP1 is expressed in the ONL of wildtype mice (arrow), but only rare AQP1-positive structures were observed in *Dlx5* mutants (arrowhead). **F,G:** The lamina propria in *Dlx5* wildtype mice (**F**) has AQP1 IR levels that are comparable to mutants (**G**). LP, lamina propria; NS, nasal septum; OE, olfactory epithelium. Scale bars = 100 μ m in **A,B,C**; 50 μ m in **D,E**, and **F,G**.

2003; Levi et al., 2003). Therefore, as a final test to confirm that AQP1-expressing cells in the lamina propria and olfactory bulb are OEG, we compared the distribution of AQP1 immunoreactivity in the olfactory bulbs and nasal cavities of wildtype and *Dlx5*^{-/-} mice (Long et al., 2003). When we compared AQP1 expression in the E18.5 wildtype and *Dlx5* mutant nasal cavities, we found that both genotypes contained strong AQP1 IR in the lamina propria (Fig. 7A,C,F,G), despite the significant irregularities of the nasal turbinates of mutants (Fig. 7C). Evidence from β -tubulin/AQP1 double-labeling experiments indicates that ORN axons fasciculate in these mutants and AQP1-positive structures associate with the fascicles (data not shown). In wildtype olfactory bulbs we detected AQP1 IR in the ONL (Fig. 7A,D, arrow), but in *Dlx5* mutant bulbs the ONL was absent and only a few isolated immunopositive structures were observed (Fig. 7B,E, arrowhead). The near absence of AQP1 in *Dlx5* mutant olfactory bulbs that lack OEG is consistent with our findings that peripheral and central OEG both express AQP1.

DISCUSSION

AQP1 expression as a unique characteristic of OEG

In this study we examined the distribution of the AQP1 water channel in the olfactory bulb and lamina propria of

embryonic and adult mice. Based on the colocalization studies, we conclude that AQP1 is expressed in olfactory ensheathing glia and is excluded from olfactory receptor neurons, astrocytes, and periglomerular cells. Expression of AQP1 is, therefore, a characteristic of OEG that distinguishes them from other CNS cell types.

Functional contribution of AQP1 in OEG

Aquaporins are found throughout the body, in cell populations specialized for rapid transmembrane water fluxes. Here we have demonstrated that AQP1 is concentrated in the outer two layers of the olfactory bulb, an area not previously known to contain cells with enhanced water transport. We also demonstrate that AQP1-expressing cells are OEG, a glial subtype present in both the CNS and PNS and that displays migratory abilities and supports axonal outgrowth. Because AQP1 is not normally found in other CNS-residing glia, these water channels may contribute to the specialized features of OEG.

Of the 13 mammalian aquaporins known, only AQP4 has been described in CNS glia. Specifically, AQP4 is expressed in astrocytes, predominantly within the perivascular and subpial endfeet (Nielsen et al., 1997), areas that also are enriched for Kir4.1, a potassium channel involved in the clearance of extracellular K⁺ from active neurons (Nagelhus et al., 1999). Studies indicate that extracellular K⁺ is taken up by astrocytes and directed into blood vessels or

the subarachnoid space through astrocytic endfeet. The resulting osmotic gradient induces water movement that is facilitated by AQP4 (Dietzel et al., 1980; Holthoff and Witte, 2000; Niermann et al., 2001). As a consequence, extracellular K^+ is rapidly buffered in active neuropil and ion homeostasis is maintained. Because AQP1 and AQP4 belong to the same subfamily and have similar structural and permeability characteristics, AQP1 may also contribute to the establishment of ion homeostasis in active ORNs. In support of this hypothesis, Gao et al. (2006) showed that AQP1, but not AQP4, is expressed in both myelinating and nonmyelinating Schwann cells, which suggested that these two aquaporin channels facilitate similar homeostatic goals, despite their differential expression in the PNS and CNS. That AQP1, but not AQP4, is expressed by OEG may be a reflection of their peripheral embryonic derivation and partial phenotypic similarity to Schwann cells. Therefore, one function of AQP1 in OEG may be to enhance neuronal conduction via ion-water homeostasis.

A second possibility is that AQP1 is related to OEG motility. Interestingly, highly migratory glioma cells express both AQP1 and AQP4 (Endo et al., 1999; Markert et al., 2001; McCoy and Sontheimer, 2007). Results from these studies suggest that the rapid changes in cell volume necessary for tumor cells to invade narrow spaces in tightly packed brain tissue are mediated by aquaporin-dependent water flux. Furthermore, when either AQP1 or AQP4 are reintroduced into isolated, stable glioma cell lines that have lost aquaporin expression, only those lines in which AQP1 expression was reestablished exhibit restored migratory ability (McCoy and Sontheimer, 2007). As OEG exhibit substantial migratory abilities *in vitro* and during embryonic development, their expression of AQP1 may contribute to this essential function.

OEG migration is guided by lamellipodia at the ends of the leading processes but also by “waves of lamellipodia” along the process shafts (Windus et al., 2007). Time-lapse *in vivo* and *in vitro* imaging shows a rapid expansion and retraction of lamellipodia as OEG navigate through their environment and form cell-to-cell contacts (Windus et al., 2007). Other studies report that cultured OEG can rapidly and dramatically change size, shape, and the direction of their migration (van den Pol and Santarelli, 2003). Such activity may involve water channels that facilitate quick changes in cell volume. In support of this idea, McCoy and Sontheimer (2007) found that AQP1 is expressed along lamellipodia at the leading edge of migratory glioma cells. Although more detailed studies are necessary, these observations support the hypothesis that the motility and alterations in size displayed by OEG could be regulated by AQP1-mediated water transport.

Because of the continuous turnover of ORN in the adult, OEG may be required to adjust their volume and

the size of their processes. Under normal conditions, OEG form tubular channels of long, thin cytoplasmic processes around large groups of ORN axons. To partially segregate axons into tightly packed clusters, the OEG invest additional thin sheets of cytoplasm inward (Field et al., 2003). After ORN axons undergo retrograde degeneration, they are replaced by new axons. To accommodate these changes, the longitudinal channels formed by OEG are maintained, but the thin cytoplasmic processes dramatically increase in size (Li et al., 2005). This rapid size change is likely related to the active phagocytic response of OEG and may be facilitated by AQP1-dependent water flux. When the phagocytic phase is complete, OEG processes return to their original size (Li et al., 2005), which allows for active recapture and packing of newly generated axons, and again the change in cell volume could be mediated by AQP1.

Using AQP1 as an OEG marker after spinal cord injury

Transplantation of OEG has been used as a bridge to facilitate regeneration of axons severed by spinal cord injury. Unfortunately, interpreting the results of these studies is limited by the difficulty of locating OEG *in vivo*, many months after their transplantation. We originally thought that AQP1 might reliably identify OEG following spinal cord injury, but unfortunately AQP1 is also expressed in Schwann cells (Gao et al., 2006), which enter a spinal cord injury site and must be distinguished from OEG. As interest in the reparative potential of OEG increases, it is reasonable to speculate that a better understanding of the function of AQP1 in these cells will provide valuable clues as to how OEG promote axonal repair.

ACKNOWLEDGMENTS

We thank Dr. Steve Runyan for generating the mouse OEG cultures, Tiffany Yap for technical assistance, Drs. John Rubenstein, Jason Long, and Xidao Wang for generous gifts of tissue, and Dr. John Ngai and members of his laboratory as well as Dr. Almudena Ramón-Cueto for helpful suggestions and advice.

LITERATURE CITED

- Ablimit A, Matsuzaki T, Tajika Y, Aoki T, Hagiwara H, Takata K. 2006. Immunolocalization of water channel aquaporins in the nasal olfactory mucosa. *Arch Histol Cytol* 69:1–12.
- Agre P, King LS, Yasui M, Guggino WB, Ottersen OP, Fujiyoshi Y, Engel A, Nielsen S. 2002. Aquaporin water channels—from atomic structure to clinical medicine. *J Physiol* 542: 3–16.
- Akins MR, Greer CA. 2005. Cytoskeletal organization of the developing mouse olfactory nerve layer. *J Comp Neurol* 494:358–367.

- Anderson SA, Qiu M, Bulfone A, Eisenstat DD, Meneses J, Pedersen R, Rubenstein JL. 1997. Mutations of the homeobox genes *Dlx-1* and *Dlx-2* disrupt the striatal subventricular zone and differentiation of late born striatal neurons. *Neuron* 19:27–37.
- Au WW, Treloar HB, Greer CA. 2002. Sublaminar organization of the mouse olfactory bulb nerve layer. *J Comp Neurol* 446:68–80.
- Bailey MS, Shipley MT. 1993. Astrocyte subtypes in the rat olfactory bulb: morphological heterogeneity and differential laminar distribution. *J Comp Neurol* 328:501–526.
- Britis PA, Lemmon V, Rutishauser U, Silver J. 1995. Unique changes of ganglion cell growth cone behavior following cell adhesion molecule perturbations: a time-lapse study of the living retina. *Mol Cell Neurosci* 6:433–449.
- Bulfone A, Wang F, Hevner R, Anderson S, Cutforth T, Chen S, Meneses J, Pedersen R, Axel R, Rubenstein JL. 1998. An olfactory sensory map develops in the absence of normal projection neurons or GABAergic interneurons. *Neuron* 21:1273–1282.
- Depew MJ, Liu JK, Long JE, Presley R, Meneses JJ, Pedersen RA, Rubenstein JLR. 1999. *Dlx5* regulates regional development of the branchial arches and sensory capsules. *Development* 126:3831–3846.
- Devon R, Doucette R. 1992. Olfactory ensheathing cells myelinate dorsal root ganglion neurites. *Brain Res* 589:175–179.
- Dietzel I, Heinemann U, Hofmeier G, Lux HD. 1980. Transient changes in the size of the extracellular space in the sensorimotor cortex of cats in relation to stimulus-induced changes in potassium concentration. *Exp Brain Res* 40:432–439.
- Doucette R. 1984. The glial cells in the nerve fiber layer of the rat olfactory bulb. *Anat Rec* 210:385–391.
- Doucette R. 1990. Glial influences on axonal growth in the primary olfactory system. *Glia* 3:433–449.
- Doucette R. 1993. Glial cells in the nerve fiber layer of the main olfactory bulb of embryonic and adult mammals. *Microsc Res Tech* 24:113–130.
- Endo M, Jain RK, Witwer B, Brown D. 1999. Water channel (aquaporin 1) expression and distribution in mammary carcinomas and glioblastomas. *Microvasc Res* 58:89–98.
- Field P, Li Y, Raisman G. 2003. Ensheathment of the olfactory nerves in the adult rat. *J Neurocytol* 32:317–324.
- Franceschini IA, Barnett SC. 1996. Low-affinity NGF-receptor and E-N-CAM expression define two types of olfactory nerve ensheathing cells that share a common lineage. *Dev Biol* 173:327–343.
- Franklin RJ, Gilson JM, Franceschini IA, Barnett SC. 1996. Schwann cell-like myelination following transplantation of an olfactory bulb ensheathing cell line into areas of demyelination in the adult CNS. *Glia* 17:217–224.
- Gao H, He C, Fang X, Hou X, Feng X, Yang H, Zhao X, Ma T. 2006. Localization of aquaporin-1 water channel in glial cells of the human peripheral nervous system. *Glia* 53:783–787.
- Gong Q, Shipley MT. 1996. Expression of extracellular matrix molecules and cell surface molecules in the olfactory nerve pathway during early development. *J Comp Neurol* 366:1–14.
- Gong Q, Bailey MS, Pixley SK, Ennis M, Liu W, Shipley MT. 1994. Localization and regulation of low affinity nerve growth factor receptor expression in the rat olfactory system during development and regeneration. *J Comp Neurol* 344:336–348.
- Graziadei PP, Graziadei GA. 1979. Neurogenesis and neuron regeneration in the olfactory system of mammals. I. Morphological aspects of differentiation and structural organization of the olfactory sensory neurons. *J Neurocytol* 8:1–18.
- Haan EA, Boss BD, Cowan WM. 1982. Production and characterization of monoclonal antibodies against the “brain-specific” proteins 14–3-2 and S-100. *Proc Natl Acad Sci USA* 79:7585–7589.
- Halasz N, Jungdahl A, Hokfelt T, Johansson O, Goldstein M, Park D, Biberfeld P. 1977. Transmitter histochemistry of the rat olfactory bulb. I. Immunohistochemical localization of monoamine synthesizing enzymes. Support for intrabulbar, periglomerular dopamine neurons. *Brain Res* 126:455–474.
- Holthoff K, Witte OW. 2000. Directed spatial potassium redistribution in rat neocortex. *Glia* 29:288–292.
- Huber LJ, Chao MV. 1995. Mesenchymal and neuronal cell expression of the p75 neurotrophin receptor gene occur by different mechanisms. *Dev Biol* 167:227–238.
- Jahed A, Rowland JW, McDonald T, Boyd JG, Doucette R, Kawaja MD. 2007. Olfactory ensheathing cells express smooth muscle α -actin in vitro and in vivo. *J Comp Neurol* 503:209–223.
- King LS, Kozono D, Agre P. 2004. From structure to disease: the evolving tale of aquaporin biology. *Nat Rev Mol Cell Biol* 5:687–698.
- Kosaka K, Toida K, Aika Y, Kosaka T. 1998. How simple is the organization of the olfactory glomerulus?: the heterogeneity of so-called periglomerular cells. *Neurosci Res* 30:101–110.
- Kubasak MD, Jindrich DL, Zhong H, Takeoka A, McFarland KC, Muñoz-Quiles C, Roy RR, Edgerton VR, Ramón-Cueto A, Phelps PE. 2008. OEG implantation and step training enhance hindlimb-stepping ability in adult spinal transected rats. *Brain* 131:264–276.
- Levi G, Puche AC, Mantero S, Barbieri O, Trombino S, Paleari L, Egeo A, Merlo GR. 2003. The *Dlx5* homeodomain gene is essential for olfactory development and connectivity in the mouse. *Mol Cell Neurosci* 22:530–543.
- Li Y, Field PM, Raisman G. 2005. Olfactory ensheathing cells and olfactory nerve fibroblasts maintain continuous open channels for regrowth of olfactory nerve fibers. *Glia* 52:245–251.
- Long JE, Garel S, Depew MJ, Tobet S, Rubenstein JL. 2003. *DLX5* regulates development of peripheral and central components of the olfactory system. *J Neurosci* 23:568–578.
- López-Vales R, Forés J, Verdú E, Navarro X. 2006. Acute and delayed transplantation of olfactory ensheathing cells promote partial recovery after complete transection of the spinal cord. *Neurobiol Dis* 21:57–68.
- Lu J, Féron F, Ho SM, Mackay-Sim A, Waite PM. 2001. Transplantation of nasal olfactory tissue promotes partial recovery in paraplegic adult rats. *Brain Res* 889:344–357.
- Lu J, Féron F, Mackay-Sim A, Waite PM. 2002. Olfactory ensheathing cells promote locomotor recovery after delayed transplantation into transected spinal cord. *Brain* 125:14–21.
- Ma T, Yang B, Gillespie A, Carlson EJ, Epstein CJ, Verkman AS. 1998. Severely impaired urinary concentrating ability in transgenic mice lacking aquaporin-1 water channels. *J Biol Chem* 273:4296–4299.
- Margolis FL, Tarnoff JF. 1973. Site of biosynthesis of the mouse brain olfactory bulb protein. *J Biol Chem* 248:451–455.
- Markert JM, Fuller CM, Gillespie GY, Bubien JK, McLean LA, Hong RL, Lee K, Gullans SR, Mapstone TB, Benos DJ. 2001. Differential gene expression profiling in human brain tumors. *Physiol Genomics* 5:21–33.
- Matsuzaki T, Ablimit A, Tajika Y, Suzuki T, Aoki T, Hagiwara H, Takata K. 2005. Water channel aquaporin 1 (AQP1) is

- present in the perineurium and perichondrium. *Acta Histochem Cytochem* 38:37–42.
- Matus A, Mughal S. 1975. Immunohistochemical localisation of S-100 protein in brain. *Nature* 258:746–748.
- McCoy E, Sontheimer H. 2007. Expression and function of water channels (aquaporins) in migrating malignant astrocytes. *Glia* 55:1034–1043.
- Miragall F, Kadmon G, Schachner M. 1989. Expression of L1 and N-CAM cell adhesion molecules during development of the mouse olfactory system. *Dev Biol* 135:272–286.
- Mizrahi A, Lu J, Irving R, Feng G, Katz LC. 2006. In vivo imaging of juxtglomerular neuron turnover in the mouse olfactory bulb. *Proc Natl Acad Sci USA* 103:1912–1917.
- Monti-Graziadei GA, Margolis FL, Harding JW, Graziadei PP. 1977. Immunocytochemistry of the olfactory marker protein. *J Histochem Cytochem* 25:1311–1316.
- Mullen RJ, Buck CR, Smith AM. 1992. NeuN, a neuronal specific nuclear protein in vertebrates. *Development* 116:201–211.
- Nagelhus EA, Horio Y, Inanobe A, Fujita FM, Nielsen S, Kurauchi Y, Ottersen OP. 1999. Immunogold evidence suggests that coupling of K⁺ siphoning and water transport in rat retinal Müller cells is mediated by a coenrichment of Kir4.1 and AQP4 in specific membrane domains. *Glia* 26:47–54.
- Nakamura Y, Lee S, Haddox CL, Weaver EJ, Lemmon VP. 2010. Role of the cytoplasmic domain of the L1 cell adhesion molecule in brain development. *J Comp Neurol* 518:1113–1132.
- Nielsen S, Smith BL, Christensen EI, Agre P. 1993. Distribution of the aquaporin CHIP in secretory and resorptive epithelia and capillary endothelia. *Proc Natl Acad Sci USA* 90:7275–7279.
- Nielsen S, Nagelhus EA, Amiry-Mogfaddam M, Bourque C, Agre P, Ottersen OP. 1997. Specialized membrane domains for water transport in glial cells: high-resolution immunogold cytochemistry of aquaporin-4 in rat brain. *J Neurosci* 17:171–180.
- Niermann H, Amiry-Mogfaddam M, Holthoff K, Witte OW, Ottersen OP. 2001. A novel role of vasopressin in the brain: modulation of activity-dependent water flux in the neocortex. *J Neurosci* 21:3045–3051.
- Pixley SK. 1992. The olfactory nerve contains two populations of glia, identified both in vivo and in vitro. *Glia* 5:269–284.
- Qiu M, Bulfone A, Martinez S, Meneses JJ, Shimamura K, Pedersen RA, Rubenstein JLR. 1995. Null mutation of *Dlx-2* results in abnormal morphogenesis of proximal first and second branchial arch derivatives and abnormal differentiation in the forebrain. *Genes Dev* 9:2523–2538.
- Qiu M, Bulfone A, Ghattas I, Meneses JJ, Christensen L, Sharpe PT, Presley R, Pedersen RA, Rubenstein JLR. 1997. Role of the *Dlx* homeobox genes in proximodistal patterning of the branchial arches: mutations of *Dlx-1*, *Dlx-2*, and *Dlx-1*, and *-2* alter morphogenesis of proximal skeletal and soft tissue structures derived from the first and second arches. *Dev Biol* 185:165–184.
- Raisman G. 2001. Olfactory ensheathing cells—another miracle cure for spinal cord injury? *Nat Rev Neurosci* 2:369–374.
- Ramón-Cueto A, Avila J. 1997. Differential expression of microtubule-associated protein 1B phosphorylated isoforms in the adult rat nervous system. *Neuroscience* 77:485–501.
- Ramón-Cueto A, Avila J. 1998. Olfactory ensheathing glia: properties and function. *Brain Res Bull* 46:175–187.
- Ramón-Cueto A, Plant GW, Avila J, Bunge MB. 1998. Long-distance axonal regeneration in the transected adult rat spinal cord is promoted by olfactory ensheathing glia transplants. *J Neurosci* 18:3803–3815.
- Ramón-Cueto A, Cordero MI, Santos-Benito FF, Avila J. 2000. Functional recovery of paraplegic rats and motor axon regeneration in their spinal cords by olfactory ensheathing glia. *Neuron* 25:425–435.
- Runyan SA, Phelps PE. 2009. Mouse olfactory ensheathing glia enhance axon outgrowth on a myelin substrate in vitro. *Exp Neurol* 216:95–104.
- Runyan SA, Roy R, Zhong H, Phelps PE. 2005. L1 CAM expression in the superficial dorsal horn is derived from the dorsal root ganglion. *J Comp Neurol* 485:267–279.
- Shantheraveerappa TR, Bourne GH. 1962. The ‘perineural epithelium,’ a metabolically active, continuous, protoplasmic cell barrier surrounding peripheral nerve fasciculi. *J Anat* 96:527–537.
- Shields SD, Mazario J, Skinner K, Basbaum AI. 2007. Anatomical and functional analysis of aquaporin 1, a water channel in primary afferent neurons. *Pain* 131:8–20.
- Thomas PK. 1963. The connective tissue of peripheral nerve: an electron microscope study. *J Anat* 97:35–44.
- Tóth ZE, Mezey E. 2007. Simultaneous visualization of multiple antigens with tyramide signal amplification using antibodies from the same species. *J Histochem Cytochem* 55:545–554.
- Valverde F, Santacana M, Heredia M. 1992. Formation of an olfactory glomerulus: morphological aspects of development and organization. *Neuroscience* 49:255–275.
- van den Pol AN, Santarelli JG. 2003. Olfactory ensheathing cells: time lapse imaging of cellular interactions, axonal support, rapid morphologic shifts, and mitosis. *J Comp Neurol* 458:175–194.
- Windus LC, Claxton C, Allen CL, Key B, St John JA. 2007. Motile membrane protrusions regulate cell-cell adhesion and migration of olfactory ensheathing glia. *Glia* 55:1708–1719.